Finite Element Analysis of Wirelessly Interrogated Implantable Bio-MEMS

Don W. Dissanayake[a,b], Said F. Al-Sarawi[a,b], Tien-Fu Lu[c] and Derek Abbott[a,b,d]

[a]Centre for High Performance Integrated Technologies and Systems (CHiPTec), University of Adelaide, SA 5005, Australia
[b]School of Electrical and Electronic Engineering, University of Adelaide, SA 5005, Australia
[c]School of Mechanical Engineering, University of Adelaide, SA 5005, Australia
[d]Centre of Biomedical Engineering (CBME), University of Adelaide, SA 5005, Australia

ABSTRACT

Wirelessly interrogated bio-MEMS devices are becoming more popular due to many challenges, such as improving the diagnosis, monitoring, and patient wellbeing. The authors present here a passive, low power and small area device, which can be interrogated wirelessly using a uniquely coded signal for a secure and reliable operation. The proposed new approach relies on converting the interrogating coded signal to surface acoustic wave that is then correlated with an embedded code. The suggested method is implemented to operate a micropump, which consist of a specially designed corrugated microdiaphragm to modulate the fluid flow in microchannels. Finite Element Analysis of the micropump operation is presented and a performance was analysed. Design parameters of the diaphragm design were finetuned for optimal performance and different polymer based materials were used in various parts of the micropump to allow for better flexibility and high reliability.

Keywords: ANSYS, Diaphragm, Diffuser, Electrostatic, FEM, Micropump, Nozzle, SAW device

1. INTRODUCTION

Bio-MEMS (Micro Electro Mechanical Systems) devices are increasingly been developed for drug delivery and biomedical related applications. Conventional drug delivery methods such as oral tablets or injections are not effective to deliver the drug effectively within their therapeutic range as there is a sharp initial increase in drug concentration, followed by a fast decrease to a level below the therapeutic range.[1] In general, it is known that most of the drugs are effective if delivered within a specific range of concentration between the maximum and minimum desired levels. Above the maximum range, the drugs are toxic and below that range, they have no therapeutic effectiveness.[2] In applications that require high precision in delivering drugs or any other fluid, micropumps are a desired component of Bio-MEMS and microfluidic devices.[3]

1.1 Microfluidic devices and Micropumps

Vast variety of micropumps are being designed and developed by various researchers in the past.[3,4] However, for micropumps that are targeted for use as *in-vivo* applications, wireless and batteryless operation is highly desired. In these low-powered micropumps, the functionality of the diaphragm and the flow resistant modules are equally important since these components determine the fluid flow characteristics of the device. Additionally, microdimensions and material properties are of great importance in the design of such a diaphragm in order to achieve the optimal performance.

Further author information: (Send correspondence to Don W. Dissanayake)
Don W. Dissanayake: E-mail: don.dissanayake@adelaide.edu.au

Biomedical Applications of Micro- and Nanoengineering IV and Complex Systems, edited by Dan V. Nicolau, Guy Metcalfe
Proc. of SPIE Vol. 7270, 727004 · © 2008 SPIE · CCC code: 1605-7422/08/$18 · doi: 10.1117/12.814074

Downloaded From: http://proceedings.spiedigitallibrary.org/ on 11/13/2012 Terms of Use: http://spiedl.org/terms

1.2 Microdiaphragms for flow modulation

The structure of the diaphragm may be flat or corrugated depending on the intended application. Flat diaphragms are used for most of the sensing related applications. However for applications where large displacements are desired, corrugated diaphragm structures are ideally suited.[5] A corrugated diaphragm is made by forming concentric beads or corrugations on a thin sheet of metal (or a similar material). As a result, diaphragm increases in rigidity and becomes suitable for operation at larger displacements and longer linear travel than a flat diaphragm.[6]

1.3 Diffuser Elements for flow rectification

Generally, valveless micropumps are considered very attractive as they are low cost devices due to their simple structure. Interestingly, different diffuser geometries such as conical, pyramidal and flat-walled diffusers have been widely used for valveless micropumps. The choice of diffuser shape is basically dependent on the fabrication process. For planar lithography and standard micromachining fabrication techniques, flat-walled diffusers (planar diffusers) are considered to be the best choice.[7] The planar configuration of these flat-walled diffusers widens the spectrum of possible materials and pump driver designs. Moreover, the increasing use of plastics and polymer materials are foreseeable because of its low cost and good bio-compatibility and chemical resistance. Another potential advantage of the flat-walled diffuser is that, under the same inlet boundary-layer condition, the best flat-walled diffuser is comparatively shorter than the best conical design, which helps to reduce the device dimensions. Therefore, in designs where the available space is a critical design parameter, the flat-walled diffuser can be used for better performance.[7]

The designed micropump consists of two nozzle-diffuser elements that are connected through a pumping chamber which consists of an electrostatically actuated conductive diaphragm. When activated, the diaphragm periodically increases and decreases the volume of the pumping chamber. By changing the orientation of the diffuser elements such that the wide end of one is attached to the chamber on one side and the narrow end of the other is attached to the opposite side, a net pumping action across the chamber occurs (Figure 1) as the diaphragm vibrates up and down with a predefined frequency.

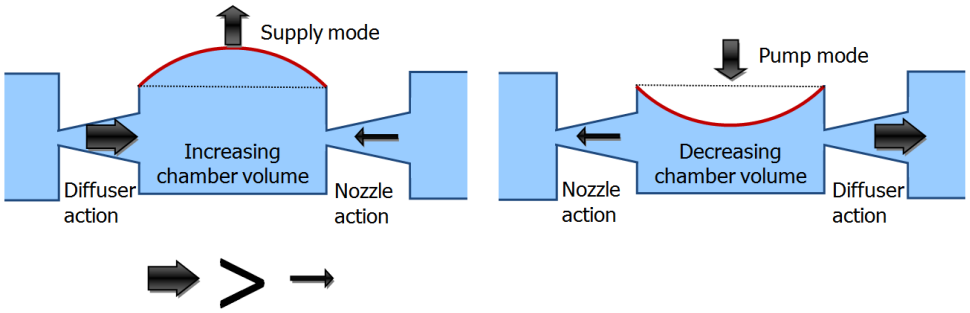

Figure 1. Illustration of the flow rectification phenomena in a valveless/diffuser micropump while the micropump is in supply mode (expansion mode) and pump mode (contraction mode). Here, thicker arrows imply a higher volume flow rate.

In this paper, to analyse the behaviour of the micropump components, Finite Element Analysis (FEA) tools are used instead of complex numerical analysis methods. Next section briefly introduces the underlying novel actuation mechanism for such a micropump device and is followed by Section 2, which highlights the significance of FEA approach in this research. Sections 3 and 4 present theoretical overviews, design and simulation results for microdiaphragm and diffuser element analysis.

Downloaded From: http://proceedings.spiedigitallibrary.org/ on 11/13/2012 Terms of Use: http://spiedl.org/terms

1.4 SAW Device Based Wireless and Secure Operation

The wireless operation is integrated to the novel micropump design with the use of a SAW (Surface Acoustic Wave) device. A secure code is embedded in to the output IDT (Inter Digital Transducer) of the SAW device for a secure operation of the the micropump. As depicted in Figure 2, the conductive diaphragm is placed on top of the output IDT of the SAW device and it is actuated electrostatically due to the generated electrostatic force between the conductive diaphragm and the output IDT.[8,9]

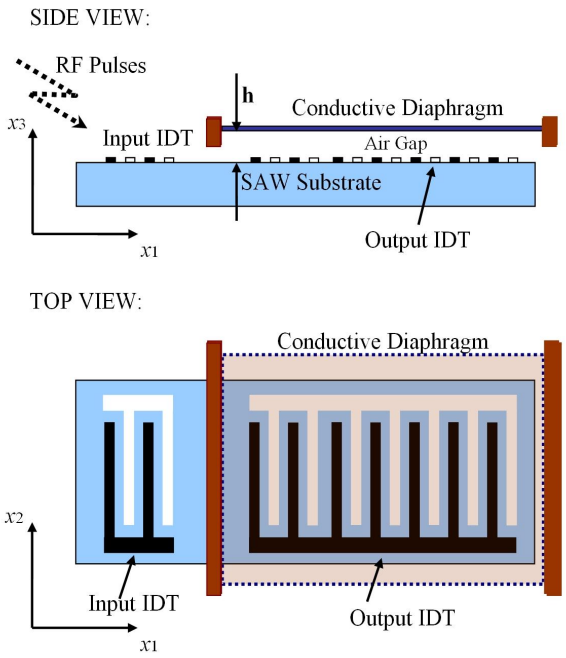

Figure 2. Side view: Air-gap separated diaphragm is placed above the output IDT of the SAW device. Top view: The area of the diaphragm is larger than the effective area of the output IDT, hence allows more deflection as the stress levels at the central area of the diaphragm is less.

2. SIGNIFICANCE IN FINITE ELEMENT ANALYSIS (FEA)

Governing equation of the transverse deflection for the microdiaphragm can be expressed as:[10,11]

$$D\nabla^4 W_D + \rho_D t_D \frac{\partial^2 W_D}{\partial t^2} = F - P, \tag{1}$$

where the bending stiffness $D = \frac{E{t_D}^3}{[12(1-\nu^2)]}$, E is the modulus of elasticity, t_D is the diaphragm thickness and ν is the Poisson ratio of the diaphragm material. Moreover, W_D is the deflection in the pump diaphragm, ρ_D is the density of the diaphragm material and ∇^4 is the two dimensional double Laplacian operator. Here, F is the actuating electrostatic force acting on the diaphragm as shown later in Equation 2, while P is the dynamic pressure imposed on the diaphragm by the fluid as shown in Equation 3.

In SAW based electrostatic actuation, the generated electrostatic force at the conductive diaphragm is a function of the instantaneous displacement of the diaphragm. In other words, since the applied electrostatic force is a function of both electric potential at the output IDT and the instantaneous gap between the diaphragm and the SAW device, the applied force F given in Equation 1 is subject to the time varying diaphragm displacement W_D. In electrostatic actuation, the electrostatic attraction force F applied on the conductive plates can be

Downloaded From: http://proceedings.spiedigitallibrary.org/ on 11/13/2012 Terms of Use: http://spiedl.org/terms

described using the parallel plate capacitor effect[2] as

$$F = \frac{\varepsilon A \Phi^2}{2y^2}, \tag{2}$$

where ε is the dielectric coefficient of the medium between the plates, A is the effective plate area, y is the plate spacing, which is defined as $(h - W_D)$ in x_3 direction and Φ is the applied electric potential between the plates.

As was previously reported, in the SAW based micropump, the electrostatic force is generated due to the time varying electric potential at the output IDT and the conductive diaphragm.[9,12,13] Additionally it has been shown that the electric potential at the output IDT region is a combination of both the electric potential at the IDT and the electric potential at the IDT finger gaps,[9,12] which results in a time and space dependant electrostatic force with high complexity.

In electrostatically actuated micropumps, the fluid flow is considered to be incompressible. Therefore the governing equations for fluid flow can be written as

$$\rho_L \frac{dV}{dt} = \rho_L g + \mu \nabla^2 V - \nabla P, \tag{3}$$

$$\frac{\partial \rho_L}{\partial t} + (V \cdot \nabla)\rho_L = 0, \tag{4}$$

where V is the fluid velocity vector, μ is the viscosity, ρ_L is the density and P is the dynamic pressure of the fluid. The above governing equations show that the electrostatic field between the output IDT and the diaphragm, the deflection of the diaphragm and the flow of the working fluid are always coupled during the pumping action in a electrostatically actuated valveless micropump. In order to determine the deflection of the diaphragm due to excitation force, we have to solve the Equations 1, 2 and 3 simultaneously.

However this analytical approach is quite complicated and requires extensive computational effort. Because of the complexity in analysis of electrostatic micropump, which involves electrostatic, structural and fluid field couplings in a complicated geometrical arrangement, FEA can be considered to be a sensible approach rather than an analytical system, to study the behaviour of the electrostatic micropump. Hence in this research, the FEA of microdiaphragm and diffuser design are presented and discussed with the used of the ANSYS simulation tools.[14]

3. DIAPHRAGM DESIGN

Diaphragms can be operated either as a single element or for higher sensitivity as a capsule, having two diaphragms facing one another. Similar logic is applicable when diaphragms are used as fluid flow modulators for micropumps, since higher displacements are achievable from the capsule like designs.

In this specific design, more displacement is achieved by reducing h, which is the allowable gap between the diaphragm and the SAW device (see Figure 2), as the electrostatic force is inversely proportionated to the gap between the electrodes. As depicted in Figure 2, a diaphragm with a larger area results in producing higher displacements around the central region of the diaphragm. However, the dimensions of the diaphragm should be not too large, to avoid overlapping with the input IDT.

3.1 Sinusoidal and Toroidal Corrugated Diaphragm Design

It has been suggested that the shape of the corrugation profile has little affect on the performance characteristics of the diaphragm.[6] In general, diaphragms with fine sawtooth profiles are simple to manufacture and are stable at small overloads. However, manufacture of diaphragms with deep sawtooth profiles is comparatively difficult due to the possibility of cracks developing at crests as a result of stress concentration. Whereas, the fabrication of diaphragms having sinusoidal and similar shaped corrugations needs more complex tools. However, such corrugation profiles consist of minimal stress concentrations compared to sawtooth and trapezoidal profiles. Additionally, toroidal corrugations could be fabricated easily, compared to the sinusoidal corrugations. Therefore, to determine the suitability of a corrugation profile, performance analysis for sinusoidal and toroidal profiles are conducted using ANSYS and presented in the next section.

Downloaded From: http://proceedings.spiedigitallibrary.org/ on 11/13/2012 Terms of Use: http://spiedl.org/terms

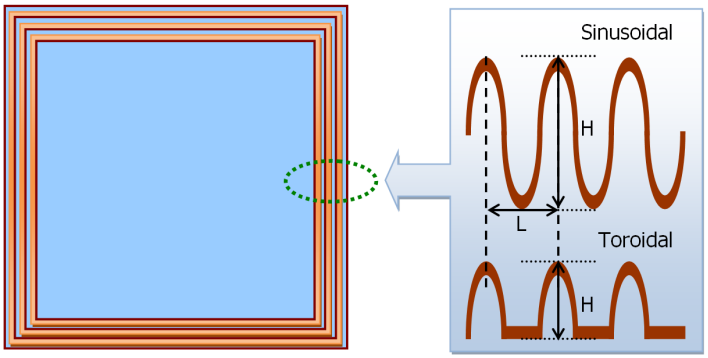

Figure 3. Sinusoidal and Toroidal corrugation profiles and corrugation parameters. Here, L denotes the corrugation wavelength and H is the corrugation height.

The parameters L and H are considered to be critical parameters in the design of the sinusoidal and toroidal corrugations as depicted in Figure 3. The ratios H/t_D, and L/H need to be carefully considered to reduce the unnecessary stress concentrations around the corrugations.[6]

3.2 Finite Element Analysis of Diaphragms

Three different scenarios are considered at the simulation level in order to compare the displacement characteristics of square shaped diaphragms, (a) a diaphragm with no corrugations (a flat diaphragm), (b) a sinusoidal corrugated diaphragm, and (c) a toroidal corrugated diaphragm. Material properties and both the electrical and mechanical boundary conditions are kept the same for all the designs, while changing only the geometry with aforementioned corrugation profiles. As it can be seen from Figure 4, the symmetry condition is exploited in order

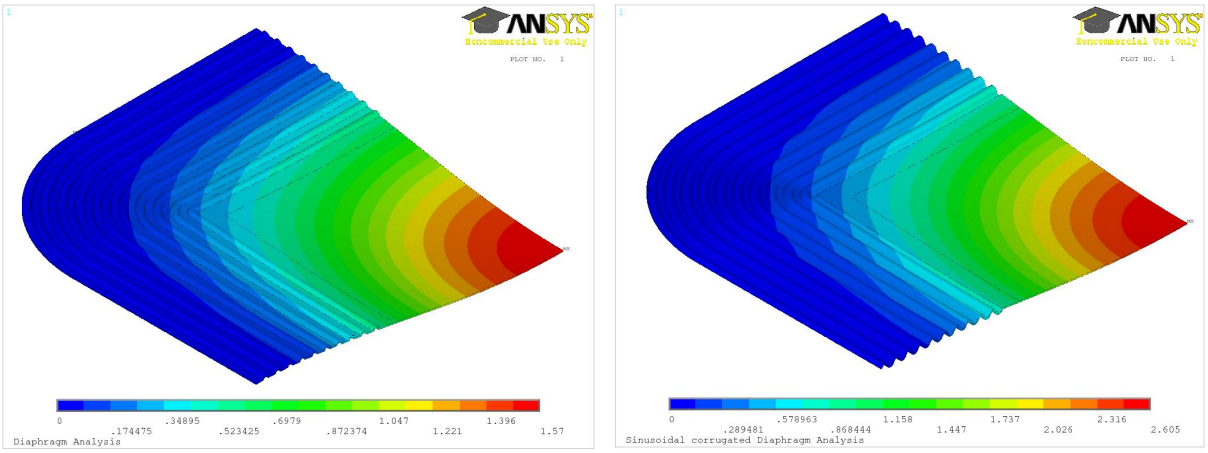

Figure 4. Finite Element Analysis (FEA) of electrostatically actuated, corrugated diaphragm design with toroidal (left) and sinusoidal (right) profiles. Quarter-symmetry is exploited to reduce the simulation time and CPU usage. Here, 10 wavelengths ($10\times L$) of corrugations are used for the analysis. Dimensions of the quarter-diaphragm segment considered are 1000 μm $\times$ 4 μm $\times$ 1000 μm (Length/2 $\times$ Thickness $\times$ Width/2).

to reduce the simulation time, while achieving a complete set of results. For the three scenarios above, quarter-symmetry is used, which means only a quarter of the design is simulated, since the square shaped diaphragm has two axes of symmetry. Displacements obtained for the above three scenarios for different input voltages are presented in Figure 5. As expected, quadratic shaped curves are observed since the relationship between the applied voltage and the displacement of the diaphragm is quadratic in nature, when the diaphragm is actuated

Downloaded From: http://proceedings.spiedigitallibrary.org/ on 11/13/2012 Terms of Use: http://spiedl.org/terms

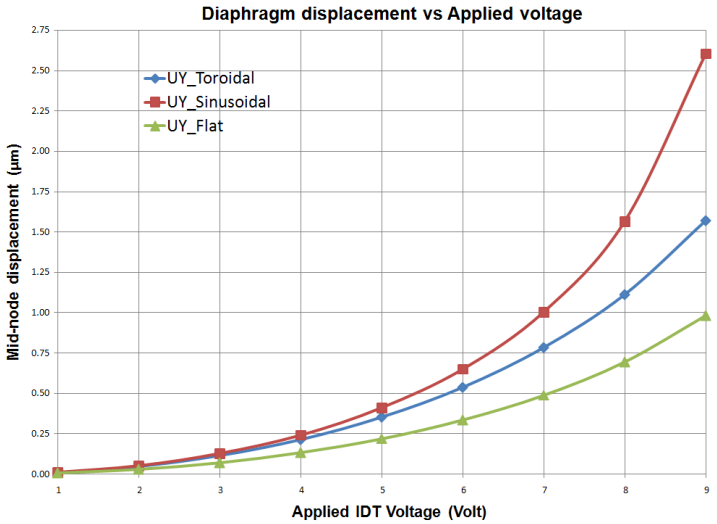

Figure 5. Comparison of displacement achieved for different corrugated diaphragms.

electrostatically.[9,15] Based on the FEA results, it is evident that a diaphragm with sinusoidal corrugations provides more deflection compared to a diaphragm with a toroidal corrugations for the same excitation voltage, and both types of diaphragms deflects more than a flat diaphragm. Hence the implementation of the sinusoidal corrugations is highly desired from the design perspective. Moreover, sinusoidal corrugations are recommended over toroidal corrugations, due to less stress concentration around the corrugations during the vibration of the diaphragm. However, as mentioned before the fabrication of the toroidal corrugations might turn out to be easier compared to sinusoidal corrugations hence the choice of the corrugation type becomes a trade off between the performance and the low cost fabrication.

4. DIFFUSER DESIGN

By definition, a diffuser element is a device for reducing the velocity and increasing the static pressure of a fluid passing through a system.[16] In view of the ease of integrating with other MEMS devices, flat-walled (planar) diffuser/nozzle elements can be employed, which has the features of square cross-section, two parallel flat walls, and two convergent flat walls. The schematic diagram (top view) of the diffuser/nozzle element is shown in Figure 6. The main geometrical parameters of the diffuser/nozzle element involve the diverging diffuser angle θ, the diffuser length $L1$ and the neck width $W1$. The flow rectification ability of the valveless micropump depends on the difference between the pressure loss in the diffuser and the nozzle directions.[10]

In the literature, several steady-flow measurements on flat-walled diffusers for micropump applications have been reported.[7] However, the experimental data are hard to be used to optimize the diffuser design for several reasons.

(i) The range of the diverging angles of the tested diffusers is very limited; the selection of the tested angles was based on the results of high Reynolds number flows and, therefore, was almost in a range of small values,

(ii) The slenderness and the inlet aspect ratio of the reported diffusers are very scattered. Additionally, it has been shown that both parameters have prominent effects on the performance of the diffuser micropump.[7,10,16]

(iii) In most experiments, the reported pressure loss was not contributed only by the diffuser but also by other components (such as inlet and outlet channels, sudden expansion and contraction, bends) which were not clearly described. Therefore, the reported data represent the total pressure loss of all the components instead of the pressure loss due to the diffuser valve solely.[7]

Due to these reasons it is important to follow a consistent design approach to analyse the diffuser elements to prevent any misinterpretation of results and findings.

Downloaded From: http://proceedings.spiedigitallibrary.org/ on 11/13/2012 Terms of Use: http://spiedl.org/terms

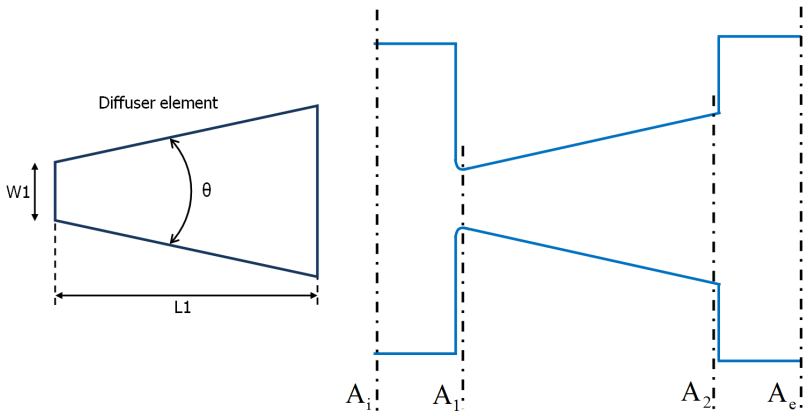

Figure 6. Top view of a flat-walled diffuser element and diffuser design parameters.

4.1 Theoretical analysis of diffuser design

It is known that the performance of a valveless micropump depends on the properties of the diffuser/nozzle elements. Hence it is important to analyse the effect of diffuser geometry in micropump operation. The pressure loss coefficient through the diffuser/nozzle elements is defined as[10]

$$K = \frac{\Delta P}{\rho_L {\upsilon_L}^2/2}, \tag{5}$$

where ΔP is the pressure drop across the diffuser direction or the nozzle direction, ρ_L is the fluid density, and υ_L is the mean flow velocity of the fluid flow at the inlet of the diffuser element. The pressure loss coefficient across the diffuser/nozzle elements is the sum of the pressure drops through the three parts, (i) the sudden contractions at the entrance, (ii) the sudden expansions at the exit, and (iii) the gradual expansions or contractions along the length of the diffuser element. Hence, the pressure loss coefficients across the diffuser direction (K_d) and the nozzle direction (K_n) are expressed as

$$K_d = K_{d,en} + K_{d,l} + K_{d,ex}\left(\frac{A_1}{A_2}\right)^2, \tag{6}$$

$$K_n = K_{n,ex} + (K_{n,l} + K_{n,en})\left(\frac{A_1}{A_2}\right)^2, \tag{7}$$

where A_1 and A_2 are respectively the narrowest and the largest areas of the diffuser/nozzle element as can be seen in Figure 6. It should be noted that the continuity theory in fluid mechanics (flow rate $=A_1\upsilon_1 = A_2\upsilon_2$) has been used in deriving K_d and K_n.

The diffuser efficiency of the diffuser/nozzle elements is defined as the ratio of the pressure loss coefficient across the nozzle direction to that in the diffuser direction;

$$\eta = \frac{K_n}{K_d}. \tag{8}$$

If the pressure loss coefficient in the nozzle direction is higher than that in the diffuser direction, that is if $\eta > 1$, a pumping action from the inlet to the outlet is caused. In contrast, $\eta < 1$ will lead to a pumping action from the outlet to the inlet (inverted). Therefore some care is needed while designing the diffuser elements in order to achieve the expected outcomes. Moreover, once the diffuser efficiency is known, the flow rectification efficiency of the valveless micropump can be expressed as

$$\varepsilon = \frac{\left|\eta^{1/2} - 1\right|}{\eta^{1/2} + 1}. \tag{9}$$

Downloaded From: http://proceedings.spiedigitallibrary.org/ on 11/13/2012 Terms of Use: http://spiedl.org/terms

Based on the above presented expressions, it is evident that the flow rectification effect of the device depends on the diffuser geometry. Additionally, dimensional analysis of a flat-walled diffuser shows that, for incompressible flow, the performance of the diffuser depends mainly upon Reynolds number, inlet boundary-layer blockage factor (the ratio of the effective area displaced by the inlet boundary layer to the diffuser inlet area), aspect ratio, and two of the three (dependent) geometrical parameters, namely the diverging angle, the slenderness, and the area ratio.[7]

The boundary-layer blockage factor at A_1 (refer Figure 6) depends on the relative length of the upstream duct and has significant effects on the performance of the diffuser.[7] It has also been shown that the velocity distribution at the diffuser exit A_2 is always non-uniform and the downstream duct provides a settling passage in which the kinetic energy in the distorted outflow is converted to a static pressure rise due to turbulent mixing. Therefore, at high Reynolds number, the loss for the diffuser with an outlet duct is smaller than that for the same diffuser with a free discharge and the location of A_e should be chosen in such a way that the static pressure at the exit P_e achieves a maximum.[7] Therefore care is taken in defining the distance between A_i and A_1 (also A_2 and A_e) during the FEA of the diffusers by selecting an appropriate ratio between these distances and the diffuser length.

4.2 Finite Element Analysis of flat-walled diffusers

Flat-walled diffuser elements were designed and analysed using ANSYS CFD (Computational Fluid Dynamics) tools.[14] For simplicity, two dimensional models were analysed for different flat-walled diffuser geometries, by varying the parameters, θ, $L1$ and $W1$. A laminar flow analysis is carried out by setting the fluid velocity at the diffuser walls to zero ($Vx = 0$ and $Vy = 0$). Considering the values used in the published literature, a pressure gradient (0 – 100 kPa) is set across the diffuser by setting inlet and outlet pressure boundary conditions. Properties of water is considered for the fluid filled in the diffusers.

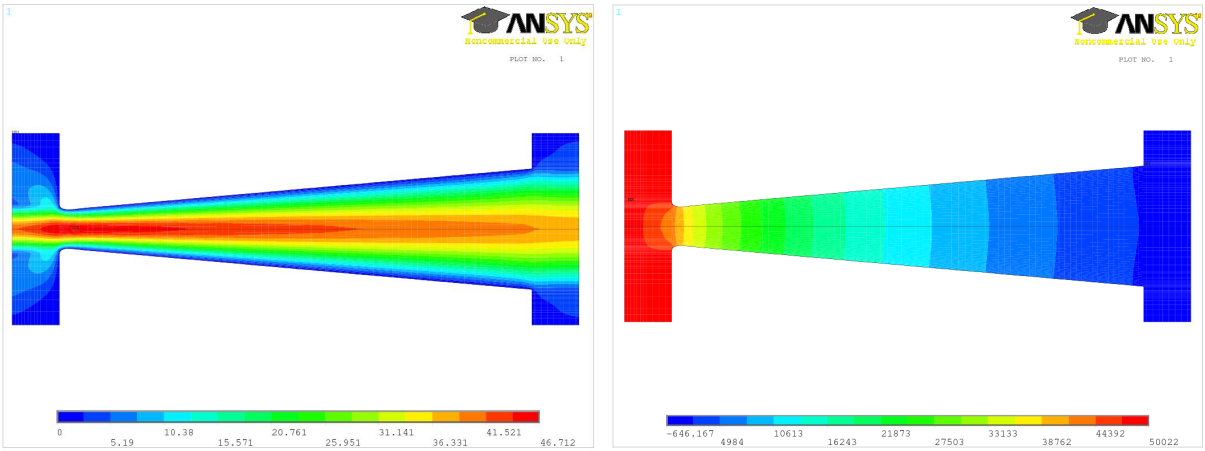

Figure 7. Flow patterns (left) and pressure distribution (right) for a two-dimensional model of a flat-walled diffuser element. Diffuser length $L1 = 1000$ μm, neck width $W1 = 80$ μm and the diverging angle $\theta = 10$ degrees.

Figure 7 shows the resulting contour plots of the velocity and pressure distribution across the diffuser element. The velocity around the inlet is larger compared to the other parts of the diffuser and the since this depicts the diffuser effect, the pressure is higher around the inlet compared to the exit of the diffuser.

Based on the 3D plot shown in Figure 8 (Left), it is apparent that the inlet velocity is larger around the center area of the inlet and also velocity increases as the pressure drop is increased.

The variation of the inlet velocity for different neck widths $W1$ is analysed for different pressure drops and the results are presented in Figure 8 (Right). According to the analysis, as the neck width increases from 40 μm to 100 μm, the inlet velocity increases for respective pressure drops. Therefore for higher flow rates, larger neck widths are desired.

Downloaded From: http://proceedings.spiedigitallibrary.org/ on 11/13/2012 Terms of Use: http://spiedl.org/terms

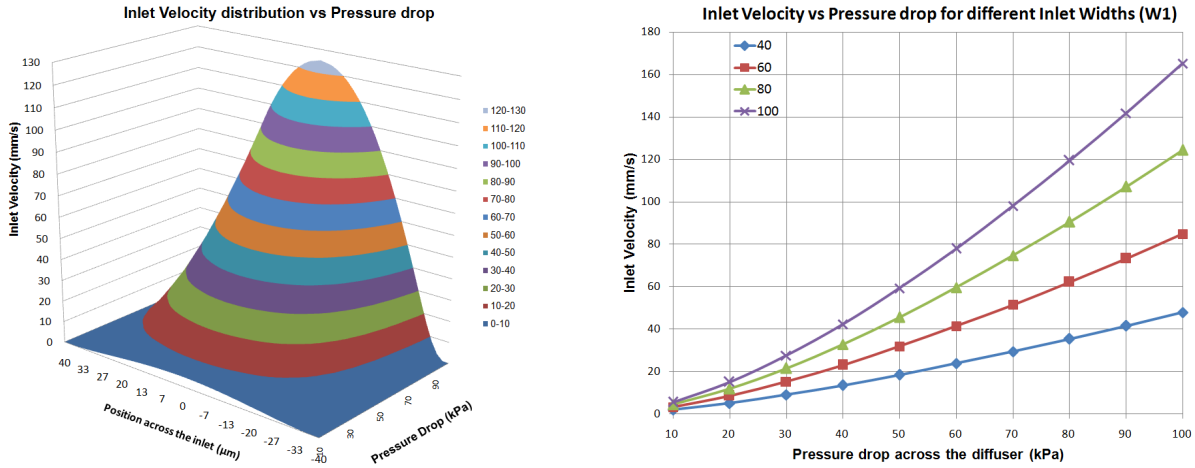

Figure 8. Left: Inlet velocity variation for different pressure drops across the inlet neck width $W1$. Right: Inlet velocity variation for different pressure drops across the diffuser for different diffuser neck widths.

In order to verify the effect of diverging angle on the flow rate, the variation of the inlet velocity for different diffuser angles θ is analysed for different pressure drops and the results are shown in Figure 9 (Left). Here, as the diffuser angle increases from 7.5 degrees to 15 degrees, the inlet velocity increases for respective pressure drops.

Finally, the variation of the inlet velocity for different diffuser lengths $L1$ is analysed in ANSYS for different pressure drops and the results are shown in Figure 9 (Right). As the diffuser length increases from 500 μm to 1250 μm, the inlet velocity decreases for respective pressure drops. Therefore for higher flow rates, shorter diffusers are desired. Based on these FEA results the optimal diffuser parameters can be selected to facilitate optimal operational conditions for flow rectification. However, the effect of the Reynolds number on the fluid flow is also need to be considered, to have a laminar flow instead of a turbulent flow, which would strongly depend on the specific application.

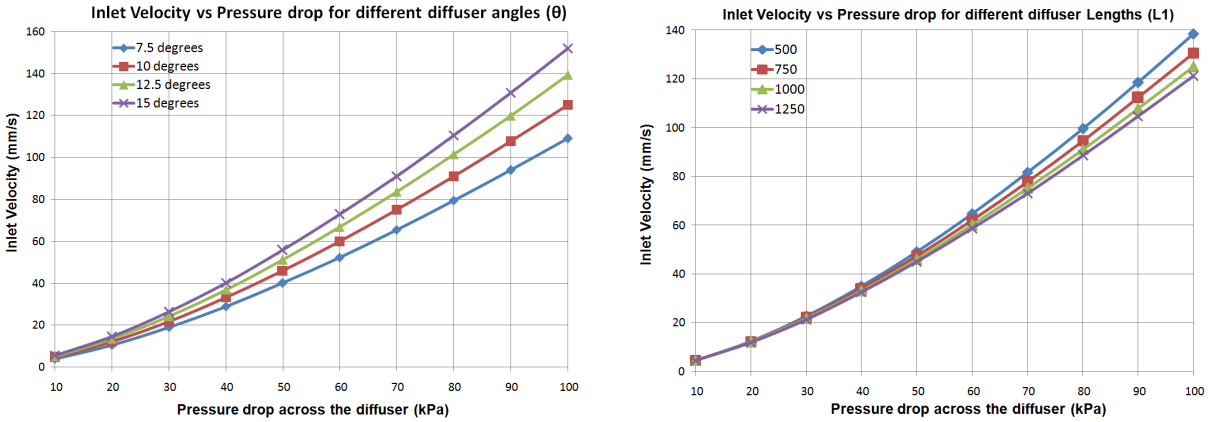

Figure 9. Left: Inlet velocity variation for different pressure drops across the diffuser for different diffuser angles. Right: Inlet velocity variation for different pressure drops across the diffuser for different diffuser lengths.

5. CONCLUSION

FEA of microdiaphragms and flat-walled diffuser elements for microfluidic devices is presented in this paper. Theoretical analysis are presented to highlight the importance in FEA to simulate and analyse complex scenarios, as an alternative option to numerical analysis. The effects of different corrugation profiles for diaphragms are

Downloaded From: http://proceedings.spiedigitallibrary.org/ on 11/13/2012 Terms of Use: http://spiedl.org/terms

illustrated and different scenarios are analysed to highlight that corrugated diaphragms achieve higher displacement over flat diaphragms for the same electrostatic field. Moreover, the effectiveness of the flat-walled diffusers are highlighted. It is demonstrated that there are several factors which directly contribute in achieving better performance of the diffuser elements for flow rectification.

The results of this research leads to the identification of important areas for further improvement of the diaphragm performance as well as the diffuser operation, hence the micropump performance under low-power conditions for Bio-MEMS related applications. With the use of multiple code coupling method in ANYS Multi-Field Solver (MFX) combined with ANSYS-CFX, a complete electrostatic-structure-fluid interaction problem can be developed and simulated to optimise the design parameters of the desired micropump.

ACKNOWLEDGMENTS

The authors would like to thank the Australian Research Council (ARC) and the School of Electrical and Electronic Engineering, The University of Adelaide, Australia, for providing the necessary funding, facilities and the support to carry out this research.

REFERENCES

[1] A. Nisar, N. Afzulpurkar, B. Mahaisavariya and A. Tuantranont, "Multifield analysis of a piezoelectrically actuated valveless micropump," *Sensors and Transducers Journal* **94**, pp. 176–195, July 2008.

[2] N. C. Tsai, C. Y. Sue, "Review of MEMS-based drug delivery and dosing systems," *Sensors and Actuators A* **134**, pp. 555–564, 2007.

[3] W. Wang and S. A. Soper, *Bio-MEMS Technologies and Applications*, CRC Press, New York, 2007.

[4] N. T. Nguyen, X. Huang and T. K. Chuan, "MEMS-Micropumps: A review," *Transactions of the ASME Journal of Fluids Engineering* **124**, pp. 384–392, June 2002.

[5] C. S. Rangan, G. R. Sarma and V. S. V. Mani, *Instrumentation Devices and Systems*, Tata McGraw-Hill Pub. Comp. Ltd., New Delhi, 1983.

[6] M. D. Giovanni, *Flat and Corrugated Diaphragm Design Handbook*, Marcel Dekker Inc., New York, 2 ed., 1982.

[7] Y. C. Wang, J. C. Hsu, P. C. Kuo and Y. C. Lee, "Loss characteristics and flow rectification property of diffuser valves for micropump applications," *International Journal of Heat and Mass Transfer* **In Press, Corrected Proof**, pp. –, July 2008.

[8] D. W. Dissanayake, S. Al-Sarawi and D. Abbott, "Corrugated micro-diaphragm analysis for low-powered and wireless Bio-MEMS," *3rd International Conference on Sensing Technology* , November 2008.

[9] D. W. Dissanayake, S. Al-Sarawi and D. Abbott, "Surface acoustic wave device based electrostatic actuator for microfluidic applications," *2nd International Conference on Sensing Technology* , pp. 381–386, November 2007.

[10] M. N. Horenstein, J. A. Perreault and T. G. Bifano, "Simulation and optimization of a piezoelectric micropump for medical applications," *The International Journal of Advanced Manufacturing Technology* **36**, pp. 516–524, March 2008.

[11] B. Lee and E.S. Kim, "Analysis of partly-corrugated rectangular diaphragms using the Rayleigh-Ritz method," *Journal of Microelectromechanical Systems* **9**, pp. 399–406, September 2000.

[12] D. W. Dissanayake, S. F. Al-Sarawi and D. Abbott, *Smart Sensors and Sensing Technology*, vol. 20, ch. Electrostatic micro actuator design using surface acoustic wave devices, pp. 139–151. Springer-Verlag, July 2008.

[13] D. W. Dissanayake, S. Al-Sarawi, Tien-Fu Lu and D. Abbott, "Design and characterisation of micro-diaphragm for low power drug delivery applications," *Proc. of SPIE–Active and Passive Smart Structures and Integrated Systems* **6928**, pp. 6928P: 1–8, April 2008.

[14] ANSYS Incorporation, "Home page." visited on 23/11/2008.

[15] M. N. Horenstein, J. A. Perreault and T. G. Bifano, "Differential capacitive position sensor for planar MEMS structures with vertical motion," *Sensors and Actuators* **80**, pp. 53–61, 2000.

[16] A. Olsson, G. Stemme and E. Stemme, "Numerical and experimental studies of flat-walled diffuser elements for valve-less micropumps," *Sensors and Actuators* **84**, pp. 165–175, August 2000.

Downloaded From: http://proceedings.spiedigitallibrary.org/ on 11/13/2012 Terms of Use: http://spiedl.org/terms